The Astrophysical Journal, 602:1075–1078, 2004 February 20

MEASUREMENT OF THE METASTABLE LIFETIME FOR THE $2s^2 2p^2\ ^1S_0$ LEVEL IN O^{2+}

Steven J. Smith,[1] I. Čadež,[1,2] A. Chutjian,[1] and M. Niimura[1]

Received 2002 January 23; accepted 2003 October 30

ABSTRACT

The radiative lifetime of the $2s^2 2p^2\ ^1S_0$ level in O^{2+} has been measured via the magnetic-dipole (M1) transition $2s^2 2p^2\ ^1S_0 \rightarrow\ ^3P_1$ at 232.17 nm. Data were recorded in a Kingdon trap, with the source of ions a 14 GHz electron cyclotron resonance ion source. The lifetime of the $^1S_0$ level was found to be 540 ± 27 ms. This is in good agreement with a previous measurement and with a number of theoretical calculations. Metastable lifetimes, when combined with collisional excitation rates, can provide a diagnostic for electron density N_e in a stellar or solar plasma.

Subject headings: atomic data — atomic processes

1. INTRODUCTION

Transitions in the O^{2+} ion are detected in a variety of astrophysical objects at wavelengths from the λ88400 nm ground-state fine-structure transition detected by the *Infrared Space Observatory* (*ISO*) in the interstellar medium (Hunter et al. 2001) to the visible spectrum, in which the ratio of the transition intensities λ436.3 nm/λ500.7 nm is used as a diagnostic of gas temperature in AGNs (Nagao, Murayama, & Taniguchi 2001) and the [O III] λ 500.7 nm transition intensity is used to map out Galactic regions of highly ionized gas (Martin & Kern 2001).

Electron temperatures and densities may be deduced from line-intensity ratios through the standard expression for the population balance among the relevant levels, which takes into account the rate of change of the population of a given level by considering all radiative and collisional transitions with interconnecting levels. This procedure can be useful insofar as the underlying Einstein A values for emission, or the cross sections for electron-impact excitation, are accurately known. If one observes in an astronomical plasma two optical transitions, the first an allowed transition from an upper level k to the ground state g and the second a forbidden transition from a metastable level i to g, then the ratio R of these intensities can serve as a diagnostic of the plasma electron density N_e and possibly of the electron temperature T_e (Keenan 1993; Chutjian 2003). This intensity ratio R is given in terms of the atomic parameters as

$$R = \frac{E_k}{E_i}\frac{C_{gk}}{C_{gi}}\left(1 + \frac{N_e C_{im}}{A_{ig}}\right), \qquad (1)$$

where E_k and E_i are energies above the ground state g. The parameters C_{gi} and C_{gk} are collisional excitation rates ($cm^3\ s^{-1}$) for exciting levels i and k, respectively, and C_{im} is the collisional depopulation rate of the metastable level i to some other level m. In equation (1), we use the fact that the optically connected level k is in coronal equilibrium. The metastable transition rate A_{ig} is related to the mean level lifetime $\tau(i)$ by the usual sum over all decay routes from level i to lower levels l (including the ground state g), $\tau(i)^{-1} = \sum_{l=i}^{N} A_{il}$. As noted by Keenan (1993), equation (1) can serve as a diagnostic of N_e for a plasma when $N_e C_{im} \gtrsim A_{ig}$.

The present work is part of a series of measurements of lifetimes of metastable levels in multiply and highly charged positive ions. Previous lifetime measurements in C^+ yielded separate A values for three sublevel transitions in the $2s2p^2\ ^4P_{1/2,3/2,5/2} \rightarrow 2s^2 2p\ ^2P^0_{1/2,3/2,5/5}$ system (Smith, Chutjian, & Greenwood 1999). Reported herein is the measurement of the lifetime of the $2s^2 2p^2\ ^1S_0$ level in O^{2+}. These data, when combined with absolute excitation cross sections for O^{2+} (Niimura, Smith, & Chutjian 2002), can provide benchmark values for assessing results of theoretical calculations carried out over a wider electron energy range.

2. EXPERIMENTAL METHODS

A partial energy level diagram of the four $2s^2 2p^2\ ^1S_0$ and $^3P_{0,1,2}$ levels is given in Figure 1. The magnetic dipole (M1) emission corresponds to the $^1S_0 \rightarrow\ ^3P_1$ decay at 232.17 nm (Wiese & Kelleher 1999). This emission line was isolated in the present work by a narrowband interference filter, with its peak of transmission centered at 232 nm, with a 12 nm (FWHM) bandwidth. The filter rejected emission lines for the transition $^1S_0 \rightarrow\ ^1D_2$ at 436.4 nm and the transition $2s2p^3\ ^5S^0_2 \rightarrow\ ^3P_{1,2}$ at 166 nm. The rejection of the latter transition was aided by the fact that the light path to the UV multiplier phototube was through the absorbing atmosphere.

Experimental measurements were carried out using the 14 GHz electron cyclotron resonance ion source (ECRIS) at the Jet Propulsion Laboratory Highly-Charged Ion (HCI) facility (Chutjian, Greenwood, & Smith 1999). The O^{2+} ions were generated from both CO and O_2 feed gas and extracted at 2×6.4 keV from the ECRIS. After extraction, the ions were mass/charge selected using a double-focusing 90° selection magnet. After the selection magnet, the HCI beam can be directed by an electrostatic switcher into one of three beam lines for excitation, charge-exchange/X-ray emission, and lifetime measurements. In this work, the HCI beam is focused into a Kingdon electrostatic ion trap for measuring lifetimes via optical decays. No other ions of $m/q = 8$ were present in the trap, such as $^{56}Fe^{7+}$ (no trace of the ^{54}Fe isotope was detected, and the plasma chamber had been cleaned since the use of ferrocene 1 yr prior) or $^{32}S^{4+}$ (the plasma chamber had been changed since the use of CS_2 2 yr prior). A schematic diagram of the

[1] Atomic and Molecular Collisions Group, Jet Propulsion Laboratory, California Institute of Technology, 4800 Oak Grove Drive, Pasadena, CA 91109.

[2] Permanent address: Jozef Stefan Institute, 1000 Ljubljana, Slovenia.

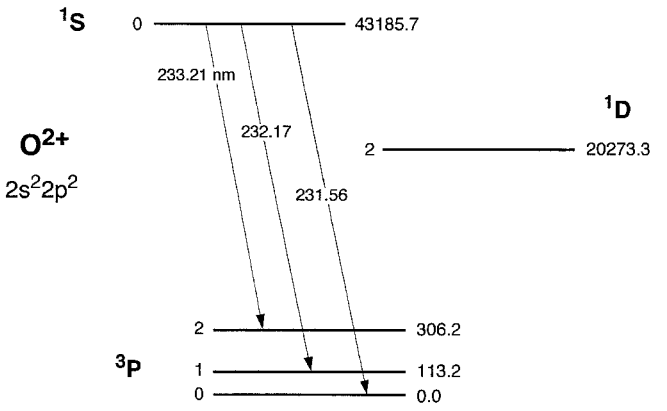

Figure 1.—Partial energy level diagram showing the $2s^2 2p^2\,{}^1S_0 \rightarrow {}^3P$ transitions in O^{2+}. Level energies are in cm^{-1}, and wavelengths are in nm.

trapping section of the beamline is given in Figure 2 of Smith et al. (1999). The complete beamline configuration (including the ECRIS, the Kingdon trap beamline, the merged-beams excitation line, and the charge-exchange/X-ray emission line) can be found in Figure 3 of Chutjian et al. (1999). Descriptions of the trap, the photon collection-detection methods, and the data acquisition procedure have been given elsewhere (Smith et al. 1999; Moehs, Church, & Phaneuf 1998).

Briefly, the O^{2+} ions are focused into the trap, after which the central wire is rapidly pulsed to a potential 3 kV below the acceleration potential of 6.4 kV. The ions settle into orbits about this wire. This relaxed ion cloud is estimated to extend over a diameter of 5–10 mm. This is much smaller than the diameter of the trap (100 mm); hence, wall collisions are minimized. While orbiting, they emit radiation at the wavelength corresponding to the energy of the transition and (in the absence of cascading into the upper level) at a decay rate given by the inverse lifetime of the upper level. Ion population in the upper level is also lost via collisional quenching, charge-exchange collisions of the HCI with the background gas, and collisions with the trap wire and walls. The photon detector and interference filter are exterior to the (fused quartz) window of the vacuum chamber. A positively biased mesh placed in front of the photon-collection optics prevents ions from hitting the first lens surface and causing fluorescence. The UV-grade, solar-blind photomultiplier is operated in a pulse-counting mode. The output pulses are amplified and counted with a PC-based multichannel scaler, with a time resolution varying from 0.1 to 10 ms per channel, depending on which part of the decay curve is being studied. The range of lifetimes that can be measured is determined at the short end by the time it takes for ions to settle into stable orbits (~1–2 ms), and at the long end by the trap lifetime (~1.7 s), which is governed by the loss mechanisms mentioned above.

3. RESULTS AND DISCUSSION

The detected photon pulses versus O^{2+} storage time are accumulated and stored in a multichannel scaler. The photon decay curves are shown in Figure 2. As in the C^+ work (Smith et al. 1999), because of the low pressure in the trap during operation (3×10^{-10} torr), there is negligible loss of population of the emitting state by ion-gas collisions. The ion radiative decay rate is given by the form $S \exp(-At)$, where S is the amplitude of the photon decay for the ${}^1S_0 \rightarrow {}^3P_1$ transition, and A its Einstein rate coefficient. The emission decay is fitted in terms of the trap decay rate $R_{\rm trap}$ by the modulating factor $\exp(-R_{\rm trap}\,t)$. The trap decay is a result of ion-surface and ion-background gas collisions. In addition, when one first loads the trap, there is an initial rapid loss of ions in the first 1–2 ms (the "settling time") from collisions of improperly loaded ions with the trap walls, the trap central wire, and ion-lens surfaces. We denote this rate by $R_{\rm set}$ and the initial number of unsuccessfully loaded ions by $B^0_{\rm set}$. Finally, there can be undesired O^{2+} ions in their ground state or another long-lived excited state(s) that are loaded into the trap. These ions will contribute to the photon "signal" as they strike the central wire, walls, or lens surfaces and emit photons into the bandpass of the detection system. This signal will decay with the characteristic trap loss rate $R_{\rm trap}$. One can then describe the experimental photon decay curve by the formula

$$F(t) = B_D + S\left(e^{-At} + I_u\right)e^{-R_{\rm trap}t} + B^0_{\rm set}e^{-R_{\rm set}t}, \qquad (2)$$

where B_D is the total number of phototube dark current counts and I_u is the fraction of (undesired) ions in their ground or other metastable, excited states.

The trap decay rate $R_{\rm trap}$ is measured independently by microchannel plates (MCP) exterior to the trap. These (non CsI-coated) plates are *insensitive* to the 230 nm photons and only respond to the positive ions in the trap. One then monitors the ion population as the trap is emptied after different elapsed trapping times, up to a maximum trapping time of 1.7 s (Smith et al. 1999). In addition, the photomultiplier signal is monitored over a longer (up to 2.0 s) time interval. This longer-term

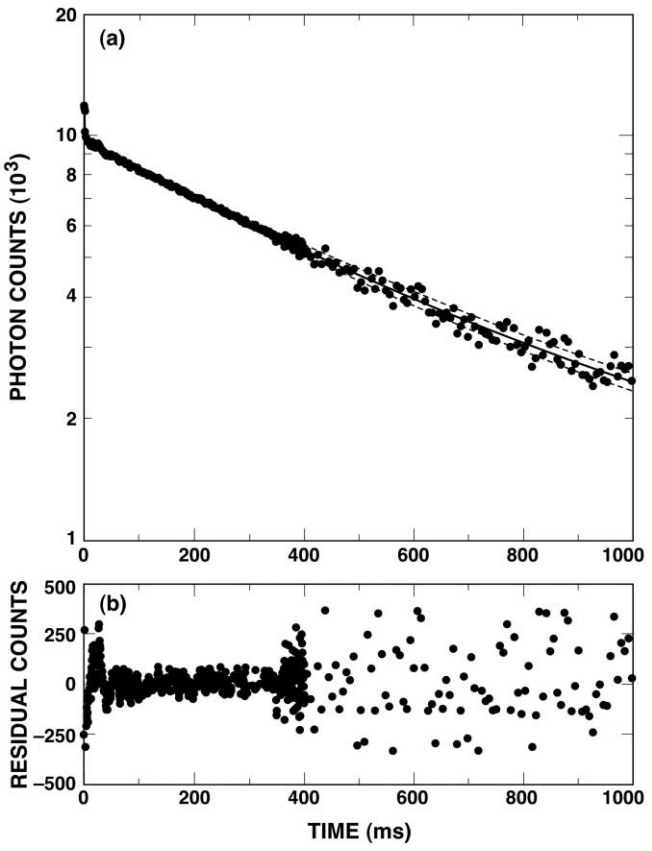

Figure 2.—Photon decay signal for the M1 232 nm decay branch in the $2s^2 2p^2\,{}^1S_0 \rightarrow {}^3P_1$ transition of O^{2+}. (*a*) Decay in the range 0–1000 ms. The best fit to the data ($\tau = 540$ ms) is shown as the solid line. Other fits used to establish the experimental error are shown as dashed lines, corresponding to $\tau = 540 \pm 27$ ms. (*b*) Residuals of the data fit in the same 0–1000 ms range.

signal arises from ion-central wire, ion-trap wall, and ion-lens surface collisions. The result of these independent techniques (i.e., ion channel using the MCP and photon channel using the phototube) gives a trap lifetime of 1750 ± 200 ms.

The trapped O^{2+} ions may also decay by collisions with the background gas. At the low trap pressures in the present work (3×10^{-10} torr), the effect of these collisions is negligible. To see this, one may assume a reasonable rate constant for the collisional removal of the $^1S_0$ level. This rate constant includes *all* effects that remove an emitting O^{2+} ion from the trap, including charge exchange, collisional deexcitation, fine-structure mixing, and collisional ejection of the ions from the trap (Church 1993). Taking a rather large rate constant of $k = 1.0 \times 10^{-8}$ cm^3 s^{-1} (see, for example, values listed in Table 7a of Church 1993) and a background gas density n in the trap of 1×10^7 cm^{-3} , one has a collisional loss rate of $kn = 0.1$ s^{-1}. This is more than 18 times smaller than the metastable decay rate of 1.85 s^{-1} and has only a small (5.6%) effect on the measured radiative decay rate. (For example, using $k = 0.7 \times 10^{-8}$ cm^3 s^{-1} reduces this correction to 3.8%.) To check the sensitivity of the lifetime to gas pressure, we admitted Ar into the trap at pressures of $3–3000 \times 10^{-10}$ torr. There was no observed effect of excited-state quenching at the lowest pressures, but quenching did become apparent in the higher part of this range. This insensitivity to added gas was also confirmed in our other unpublished measurements of lifetimes in high-charge states of Fe and Mg.

In practice, runs over several months have been carried out to improve the statistics of the exponential decay $F(t)$ [eq. (2)]. Data acquisition of the multichannel scaler card is adjusted to different time windows, as the 2048 channels of the card can be set to a range of several milliseconds to seconds. Fits are made to individual data sets. The Kingdon trap is filled and dumped once every 1.3 s. One complete data run consists of 390 fill/dump cycles of the trap. There was a total of about 290 such runs over eight days representing approximately 1.4×10^4 s of data accumulation. These data were combined with another series of runs taken months earlier, which used a 256-channel scaler. All data are shown in Figure 2 for the entire 0–1000 ms range. Shown in the insert are the residuals of the fits in the same range. One notes that there is a slight curvature to both the data and the fit. This is a consequence of the two-exponential fit described by the terms in brackets of equation (2). The fit to all data gave the following values of the parameters, with the errors at the 1 σ limit: $B_D = 1139 \pm 11.9$ counts, $S = 8566 \pm 17.6$ counts, $B^0_{\rm set} = 2760 \pm 72$ counts, $R^{-1}_{\rm set} = 2.638 \pm 0.11$ ms, and $I_u = 0.016 \pm 0.008$. Using the independently measured value $R^{-1}_{\rm trap} = 1750 \pm 200$ ms, one obtains the lifetime $\tau = A^{-1} = 540 \pm 27$ ms. Because of the large difference between the rate $R_{\rm set}$ and the rates A and $R_{\rm trap}$, the uncertainty in $R_{\rm set}$ and $B^0_{\rm set}$ does not affect the values or uncertainties in the parameters S, $R_{\rm trap}$, or A. The value of the lifetime was also checked by performing a sensitivity analysis of the fit described by equation (2). The parameters B_D, S, and $R^{-1}_{\rm trap}$ were varied within their error range. It was found that τ was most sensitive to the value of B_D. Hence the 27 ms error in τ is primarily composed of this error, and to a lesser extent the errors in S and $R^{-1}_{\rm trap}$.

One can express the goodness of fit between the function $F(t)$ and the data $d_i(t)$ by using the residuals Δ_i and the standard deviation σ_i through the expression $\Delta_i = [F(t) - d_i(t)]/\sigma_i$. Poisson statistics are used, and the σ_i are calculated from the square root of the total number of signal-plus-background counts in each time bin. The residuals converged about zero, and there was excellent agreement between data and fit with a probability distribution given by the Gaussian function $P(\Delta) = (2\pi)^{-1/2} \exp(-\Delta^2/2)$. The data-fitting procedure was performed for a number of data sets, with good statistics for each set, and with 90% of the data falling within the 90% confidence interval of $\tilde{\chi}^2$. We point out, however, such statistical agreements cannot be used to reveal systematic deviations, which might be negative for short times and positive for long times. As discussed above, the major systematic error in the present data arises from the small effect of background gas quenching. Also, the total data set and error limit herein consist of lifetimes measured over a 1 yr interval, under different beam-focusing and ECRIS-tuning conditions.

TABLE 1

THEORETICAL AND EXPERIMENTAL MEAN LIFETIMES τ (IN MS) FOR THE $2s^22p^2\ ^1S_0$ LEVEL IN O^{2+}

Theoretical	Experimental	Reference
4429		1
1269		2
559 ± 56		3
546		4
546		5
546		6
	540 ± 27	7
	530 ± 25	8
527		9
519		10
517		11
392		10

REFERENCES.—(1) Bhatia & Kastner 1993; (2) Cheng, Kim, & Desclaux 1979; (3) Galavís, Mendoza, & Zeippen 1997; (4) Garstang 1951, 1968; (5) Baluja & Doyle 1981; (6) Froese Fischer & Saha 1985; (7) this work; (8) Träbert et al. 2000; (9) Nussbaumer 1971; (10) Vilkas et al. 1996; (11) Nussbaumer & Rusca 1979.

The measured lifetime of the $2s^22p^2\ ^1S_0$ level was found to be 540 ± 27 ms at the 1 σ error limit. This compares well with the one other ion storage ring experimental measurement of 530 ± 25 (1 σ, Träbert et al. 2000). Theoretical values listed in Table 1 range from 392 to 1333 ms, 0.7 to 2.5 times the experimental values. This spread in theoretical results points out the difficulty of using theoretical data alone, which have not been verified by experimental benchmark measurements. Calculations of the intensity ratio R, as given by equation (1), can easily be incorrect by factors of four, merely from the atomic physics A_{ig} data alone. Naturally, errors in the calculated collision strengths and in the astronomical intensity observations themselves will also contribute to errors in R and N_e.

We acknowledge D. Moehs for discussions helpful to the setup and calibration of the trap and D. Church for equipment and technical discussions. I. Čadež and M. Niimura thank the National Research Council for senior fellowships through the NASA-NRC program. This work was carried out at the Jet Propulsion Laboratory, California Institute of Technology and was supported by the National Aeronautics and Space Administration.

REFERENCES

Baluja, K. L., & Doyle, J. G. 1981, J. Phys. B, 14, L11
Bhatia, A. K., & Kastner, S. O. 1993, At. Data Nucl. Data Tables, 54, 133
Cheng, K.-T., Kim, Y.-K., & Desclaux, J. P. 1979, At. Data Nucl. Data Tables, 24, 111
Church, D. A. 1993, Phys. Rep., 228, 253
Chutjian, A. 2003, in The Physics of Multiply and Highly Charged Ions, ed. F. J. Currell (Dordrecht: Kluwer), 79
Chutjian, A., Greenwood, J. B., & Smith, S. J. 1999, in Applications of Accelerators in Research and Industry, ed. J. L. Duggan & I. L. Morgan (New York: AIP), 881
Froese Fischer, C., & Saha, H. P. 1985, Phys. Scr., 32, 181
Galavís, M. E., Mendoza, C., & Zeippen, C. J. 1997, A&AS, 123, 159
Garstang, R. H. 1951, MNRAS, 111, 115
———. 1968, in IAU Symp. No. 34, Planetary Nebulae, ed. D. E. Osterbrock & C. R. O'Dell (Dordrecht: Reidel), 143
Hunter, D. A., et al. 2001, ApJ, 553, 121
Keenan, F. P. 1993, in UV and X-Ray Spectroscopy of Laboratory and Astrophysical Plasma, ed. E. Silver & S. Kahn (Cambridge: Cambridge Univ. Press), 44
Martin, C., & Kern, B. 2001, ApJ, 555, 258
Moehs, D. P., Church, D. A., & Phaneuf, R. A. 1998, Rev. Sci. Instrum., 69, 1991
Nagao, Y., Murayama, T., & Taniguchi, Y. 2001, ApJ, 546, 744
Niimura, M., Smith, S. J., & Chutjian, A. 2002, ApJ, 565, 645
Nussbaumer, H. 1971, ApJ, 166, 411
Nussbaumer, H., & Rusca, C. 1979, A&A, 72, 129
Smith, S. J., Chutjian, A., & Greenwood, J. B. 1999, Phys. Rev. A, 60, 3569
Träbert, E., Calamai, A. G., Gillaspy, J. D., Gwinner, G., Tordoir, X., & Wolf, A. 2000, Phys. Rev. A, 62, 022507
Vilkas, M. J., Martinson, I., Merkelis, G., Gaigalas, G., & Kisielius, R. 1996, Phys. Scr., 44, 281
Wiese, W. L., & Kelleher, D. E. 1999, Spectrochim. Acta B, 54, 1769